



CHORUS

This is the accepted manuscript made available via CHORUS. The article has been published as:

Effects of manganese addition on the electronic structure of BaTiO₃

J. F. Nossa, Ivan I. Naumov, and R. E. Cohen

Phys. Rev. B **91**, 214105 — Published 9 June 2015

DOI: [10.1103/PhysRevB.91.214105](https://doi.org/10.1103/PhysRevB.91.214105)

Effects of Manganese Addition on the Electronic Structure of BaTiO₃

J. F. Nossa,¹ Ivan I. Naumov,¹ and R. E. Cohen^{2,3}

¹*Extreme Materials Initiative, Carnegie Institution
for Science, Washington D.C. 20015, USA*

²*Carnegie Institution for Science, Washington D.C. 20015, USA*

³*University College London, Gower Street,
WC1E 6BT, London, United Kingdom*

Abstract

Mn is used as a dopant to improve the electromechanical properties of perovskite oxides. We investigate the effects of Mn defects and associated vacancies on the electronic and atomic properties of BaTiO₃. Using density functional theory (DFT) and DFT+U we investigate the equilibrium geometry and electronic properties of Mn ion on A or B sites, and with compensating oxygen vacancies. We study the change in the oxidation state of Mn in response to local environment changes, such as the presence of oxygen vacancies.

PACS numbers: 77.80.-e, 75.85.+t, 61.72.-y

Transition metal dopants improve the electromechanical properties of compounds like BaTiO₃, PbTiO₃ or PbZr_xTi_{1-x}O₃ (PZT),¹⁻⁹ but the origins of these effects are not well understood. Effects of the dopants can be divided into two categories, extrinsic and intrinsic. Extrinsic effects are mainly attributed to pinning of domain walls by the dopant ions and any associated oxygen vacancies. The intrinsic effects are not directly connected with domain boundary movement. They manifest themselves through the interaction between the doping induced local polarization \mathbf{P}_d and the spontaneous polarization \mathbf{P}_s . It has been proposed that defect dipoles can cooperatively align, producing a macroscopically observable internal bias field.^{5,6} One interesting intrinsic effect discussed in the literature is the possibility to increase the piezoelectric coefficients typical for PZT and Pb(Mg_{1/3}Nb_{2/3})_{1x}Ti_xO₃ (PMN-PT) by a factor of 10-40.⁷ This phenomenon has also been observed in aged BaTiO₃ samples doped with Mn.^{8,9}

Among dopants, Mn is special because it is magnetic and exhibits a variety of oxidation states (Mn²⁺, Mn³⁺ and Mn⁴⁺, and more). According to electron-spin-resonance (ESR) experiments on ABO₃ perovskites, Mn forms neutral defects and goes in the A site as Mn²⁺, in the B site as Mn⁴⁺ or as Mn²⁺ with the formation of a charge compensation complex Mn²⁺-V_O²⁻.¹⁰⁻¹⁴ In terms of Kröger-Vink notation these defects can be denoted as Mn_A[×], Mn_B[×] and (Mn_B^{''}-V_O^{••})[×], respectively, where the symbol × stands for the neutral case, ′ for net negative charge, and • for net positive charge relative to a defect-free host. When doped with Mn, the incipient ferroelectrics SrTiO₃ and KTaO₃ exhibit simultaneous spin and dipole glass behaviors with large non-linear magnetoelectric coupling.^{12,15-17} Such multiglass systems have attracted considerable attention because they can be viewed as a new class of multiferroics.

In contrast to SrTiO₃ and KTaO₃, ferroelectric BaTiO₃ doped with 3d transition metals becomes multiferroic. This was shown theoretically within the framework of spin-polarised density functional theory (DFT) computations, and experimentally by magnetization measurements.^{18,19} The ferroelectric and magnetic ordering in such 3d-metal-doped BaTiO₃ multiferroics actually compete with each other, as demonstrated in Ref. 20 by studying BaTiO₃:Mn thin films. It was found that only films with a large amount of oxygen vacancies exhibit room-temperature ferromagnetic behaviour, which was attributed to the formation of bound magnetic polarons in dilute ferromagnetic oxides.²¹

We briefly review some previous first-principles theoretical computations on defects in

oxide ferroelectrics: Yao and Fu studied the formation energies of different types of vacancies in PbTiO_3 as a function of (i) the Fermi level and (ii) chemical potentials of the atomic reservoirs.²² Cockayne and Burton computed the dipole moment of the $\text{V}_{\text{O}}^{\bullet\bullet}-\text{V}_{\text{B}}''$ divacancy and found that this moment can be twice as large as the dipole moment per cell of the bulk PbTiO_3 ; such defects, therefore, can be considered as an important source of local polarization and local fields.²³ He and Vanderbilt studied the pinning of domain walls via vacancies and revealed that the pinning effect can be strong.²⁴ Meštrić *et al.* investigated Fe^{3+} centers in PbTiO_3 and found that such centers tend to replace Ti^{4+} as acceptors and form charged defect associates $(\text{Fe}'_{\text{A}}-\text{V}_{\text{O}}^{\bullet\bullet})^{\bullet}$.²⁵ The orientation of the $(\text{Fe}'_{\text{Ti}}-\text{V}_{\text{O}}^{\bullet\bullet})^{\bullet}$ defective dipole was found to be along the c -axis parallel to the spontaneous polarization. DFT calculations for Cu impurities in PbTiO_3 found them to behave similarly to their counterpart Fe acceptor centers.²⁶ When isolated, their most stable charge state is Cu''_{Ti} , which leads to two holes in the valence band. Like Fe, the Cu centers have strong chemical driving force for association with oxygen vacancies to form $(\text{Cu}''_{\text{Ti}}-\text{V}_{\text{O}}^{\bullet\bullet})^{\times}$ defective dipoles whose preferred orientation is parallel to the polarisation, along $[001]$.²⁶ Zhang *et al.* explored the effects of acceptor substitutes on the Ti site in PbTiO_3 .²⁷ They screened group IIIB and VB elements and found that these elements favor immobile acceptor-oxygen-vacancy-acceptor defect clusters. Moreover, they found that groups IIIB and VB dopants take two distinct defect-cluster structures along the z -direction and in the xy -plane, respectively. While the former strengthens domain pinning, the latter weakens it. Rondinelli *et al.* predicted a ferroelectric ground state in BaMnO_3 .²⁸ They found that a polar ground state is stable even with non- d^0 transition metal ions. Bhattacharjee *et al.* also found that ferroelectricity and magnetism are not exclusive in CaMnO_3 .²⁹ In $\text{Sr}_{1-x}\text{Ba}_x\text{MnO}_3$, Sakai *et al.*, demonstrated that magnetic order suppresses ferroelectricity by $\sim 70\%$.³⁰ A combination of spin-phonon and polarization-strain coupling in cubic SrMnO_3 drives the system to a multiferroic ferroelectric-ferrromagnetic state.³¹

Kvyatkovskii investigated the geometry and electronic structure for defects produced by Mn impurities in SrTiO_3 and KTaO_3 .^{32,33} He used a cluster approach where the crystalline environment of the defect is modeled by a cluster that is passivated by hydrogen atoms. Kondakova *et al.* found that a Mn ion substituting for Sr in SrTiO_3 occupies an off-centered position.³⁴ This supports the idea that the observed dielectric anomalies in $\text{Sr}_{1-x}\text{Ti}_x\text{O}_3$ are due to motion of dipoles associated with off-centered Mn^{2+} impurities.¹² Using LSDA+U and many-body perturbation theory, Kizian *et al.* calculated magnetic interactions in doped

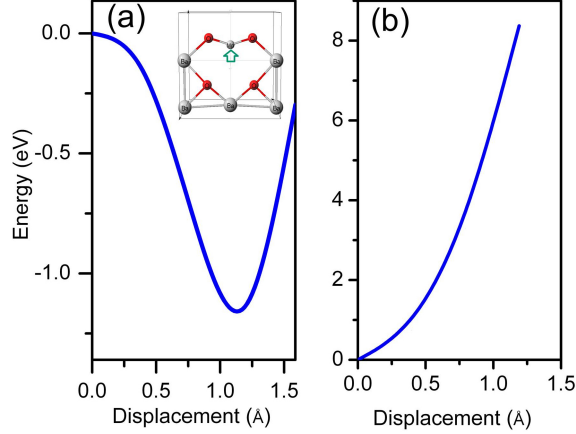


FIG. 1. Total energy dependence on the Mn (a) and Ba (b) displacements along the [001] direction in a $\text{Ba}_7\text{Ti}_8\text{MnO}_{24}$, supercell and pure BaTiO_3 , respectively. The insert shows the equilibrium position of the Mn atom in the (010) BaO plane.

SrTiO_3 between the Mn impurities of different kinds: $\text{Mn}_{\text{Sr}}^{2+}-\text{Mn}_{\text{Sr}}^{2+}$, $\text{Mn}_{\text{Sr}}^{2+}-\text{Mn}_{\text{Ti}}^{4+}$ and $\text{Mn}_{\text{Ti}}^{4+}-\text{Mn}_{\text{Ti}}^{4+}$.³⁵ They found that the exchange interaction between $\text{Mn}_{\text{Sr}}^{2+}$ impurities is significantly smaller than those for $\text{Mn}_{\text{Ti}}^{4+}$ and $\text{Mn}_{\text{Ti}}^{4+}-\text{Mn}_{\text{Ti}}^{2+}$ pairs. The authors concluded that the presence of $\text{Mn}_{\text{Sr}}^{2+}$ ions is necessary but not sufficient to explain the multiglass behaviour in Mn-doped SrTiO_3 ; the presence of $\text{Mn}_{\text{Ti}}^{4+}$ ions is also necessary.

Our calculations have been performed using a $2 \times 2 \times 2$ supercell (40 atoms plus vacancies). First, we replaced a Ti atom by a Mn ion to form a tetragonal $\text{BaTiO}_3:\text{Mn}$ structure with polarization along the z -direction. Then, we removed an oxygen atom to form a $\text{BaTiO}_3:\text{Mn}-\text{V}_\text{O}$ complex, BaTiO_3 with a Mn impurity and an O vacancy. To study the effects of the vacancy position, we also removed an oxygen atom along the x -axis. We emphasize that we want to investigate small amount of dopants, but to limit computations we use supercells ($\text{Ba}_8\text{Ti}_7\text{Mn}_1\text{O}_{23}$) containing much large concentration of Mn atoms up to 12.5%. Nevertheless, these higher concentrations are also of interest.

We have performed computations with the ABINIT code.^{36,37} Norm-conserving pseudopotentials and Projector-Augmented Wave atomic data have been first generated with OPIUM and ATOMPAW codes, and then used along with the Wu-Cohen exchange and correlation functional.³⁸ A $4 \times 4 \times 4$ Monkhorst-Pack k-point grid has been exploited for the calculation of ground state properties. For the plane-wave expansion of the valence and conduction band wave-functions, a cutoff energy of 544 eV was chosen. To compare the effects of local

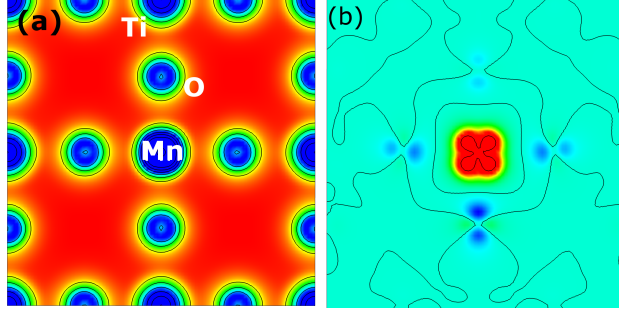


FIG. 2. (color online) The valence charge (a) and spin (b) densities around the Mn_{Ti} impurity in tetragonal BaTiO_3 in the plane parallel to the spontaneous polarization.

TABLE I. Interatomic distances, d , in pure tetragonal BaTiO_3 , with Mn_{Ti} , $\text{Mn}_{\text{Ti}}\text{-V}_{\text{O}}^z$ and $\text{Mn}_{\text{Ti}}\text{-V}_{\text{O}}^x$ defect complexes. Note that due to the breaking of cubic symmetry there are two kinds of apical (O_1 and O'_1) oxygen atoms with respect to the c -axis. In the presence of a V_{O}^x vacancy, the tetragonal symmetry is broken, so that two kinds of equatorial (two O_2 plus one O'_2) oxygen atoms can be distinguished. Labels are shown in Fig. 3. Results from DFT+U computations are shown in square brackets.

d (Å)	pure BaTiO_3	with Mn	with Mn-V_{O}^z	with Mn-V_{O}^x
$\text{Mn}(\text{Ti})\text{-O}_1$	2.234	2.199[2.124]	2.013[2.069]	2.209[2.070]
$\text{Mn}(\text{Ti})\text{-O}'_1$	1.839	1.797[1.859]	-	1.925[1.923]
$\text{Mn}(\text{Ti})\text{-O}_2$	1.984	1.952[1.961]	2.049[2.108]	2.009[1.953]
$\text{Mn}(\text{Ti})\text{-O}'_2$	1.984	1.952[1.961]	2.049[2.108]	1.894[2.082]

correlations, we have used DFT+U with $U=8$ eV and $J=0.8$ eV, as well as spin-polarised DFT. DFT+U calculations give somewhat larger ($\sim 5\%$) distances between the Mn ion and nearest O atom in the structures containing Mn-V complexes. All the structures have been optimized varying the atomic positions but taking the lattice constants, a and c , fixed to the values obtained for the pure host cubic and tetragonal lattices.

We first consider the case for a Mn impurity occupying the Ba site. We have used the pure BaTiO_3 lattice parameters in the cubic phase with $a = 3.984$ Å and in the tetragonal phase with $a = 3.968$ Å and $c = 4.073$ Å ($c/a = 1.026$). In Figure 1(a) we present the ground state energy as a function of the Mn displacement along the $[001]$ direction in the cubic phase. All the other atoms are fixed in the ideal perovskite positions. The curve

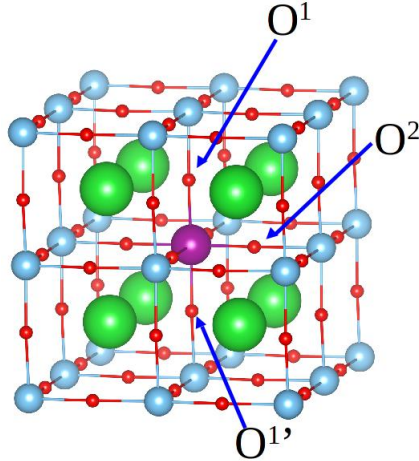


FIG. 3. (color online) Mn-doped BaTiO₃ structure. Arrows show two apical and one equatorial oxygen atoms, which are labeled as O₁, O₁' and O₂, respectively. Purple, red, blue and green balls correspond to Mn, Oxygen, Ti, and Barium atoms, respectively

has a minimum at 1.12 Å, which is twice as large as that found in SrTiO₃.³⁴ The same displacement of Ba in pure BaTiO₃, Fig. 1(b), leads to a steep rise in energy. Thus, the Mn_A impurity tends to be off-centered, like in SrTiO₃.^{32,34} This tendency is preserved going from the cubic to polar tetragonal phase. Moreover, when the tetragonal supercell with Mn_A is allowed to relax, it becomes even more tetragonal reaching a c/a ratio of 1.058, which is considerably higher than that in the defectless system (1.026).

Using DFT+U, we find that the Mn ion in the A site in the cubic structure has a magnetic moment of 5.1 μ_B suggesting that Mn_{Ba} has a spin value of 5/2. This spin value has also been found experimentally in incipient (cubic) ferroelectrics, like SrTiO₃, where Mn in the A site has a valency of 2+ and spin moment $S=5/2$.¹⁴ Decreasing U from 8.0 to 4.0 eV reduces the computed moment only slightly, to 4.5 μ_B . Magnetic moment of Mn_{Ba} also does not change much in passing from cubic to tetragonal phase whose atomic volume is significantly higher (by 4 %). So one can not expect any “magnetic collapse” in BTO:Mn_{Ba} similar to that discovered in MnO under pressure, as discussed in Ref. 39 and 40.

An Mn impurity substituting for Ti on the B site is found to be off-centered in agreement with previous work on SrTiO₃, BaTiO₃ and PbTiO₃.^{41–43} It is slightly less off-centered than Ti is in pure BaTiO₃: by 0.13 Å for Mn_{Ti} with DFT+U compared to 0.20 Å for Ti, and c/a reduces from 1.026 to 1.020 for our supercell. The Mn valence charge density is similar

to the Ti, and the spin density is concentrated mostly on the Mn ion (Fig. 2). The Mn magnetic moment is $3.38 \mu_B$ with DFT+U, suggesting that the Mn_{Ti} ion has a high spin value of $3/2$ and an oxidation state of $4+$ in this case.

We also consider two types of $\text{Mn}_{\text{Ti}}\text{-V}_{\text{O}}$ complexes containing two different kinds of nearest oxygen vacancies— V_{O}^z and V_{O}^x replacing the apical O^1 and equatorial O^2 oxygen atoms, respectively. The interatomic distances, d , in pure tetragonal BaTiO_3 and in the presence of such defects are listed in Table I. Fig. 3 shows the two apical and one equatorial oxygen atoms around Mn ion, which are labeled as O_1 , O'_1 and O_2 , respectively. We found that when the complex $\text{Mn}_{\text{Ti}}\text{-V}_{\text{O}}^z$ is introduced the tetragonal c/a is 1.020, the same as with Mn without a vacancy. **The Mn displaces towards the vacancy by about an additional 0.2 \AA compared with Ti in pure BaTiO_3 . Note that an O vacancy will generally enhance motions towards it to fill some of the missing atom's space.**

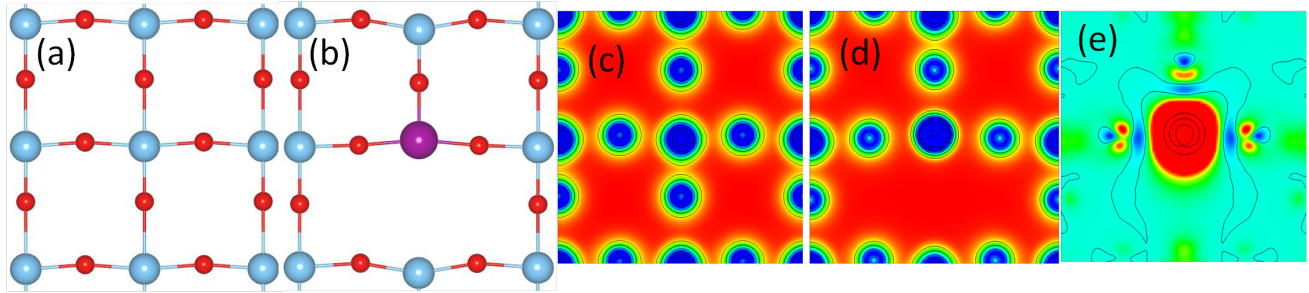


FIG. 4. (a) (color online) Undoped reference structure of BaTiO_3 . (b) $\text{Mn}_{\text{Ti}}\text{-V}_{\text{O}}$ defective associate oriented along the c -axis. Purple, red and blue balls correspond to Mn, O and Ti atoms, respectively. Note that Mn as a cation is displaced away from the oxygen vacancy due to electrostatic repulsive interaction. (c, d) Valence charge density for the structures (a) and (b). (e) Spin density for the structure (b), $\rho(r) \uparrow - \rho(r) \downarrow$.

When the defect is oriented along the c -axis or polarization direction, the displacement of the Mn ion is reduced from that of the Ti atoms in pure BaTiO_3 , as seen from Table I and Figs. 4(a) and (b). Valence charge densities for pure BaTiO_3 and $\text{BaTiO}_3\text{:Mn-V}_{\text{O}}$ are shown in Figs. 4(c) and (d), respectively. There is practically no charge density at the oxygen vacancy. The spin density (Fig. 4(e)) is centered around the Mn defect as expected, but overlaps with the neighboring O ions.

Our calculations show that in the $\text{Mn}_{\text{Ti}}\text{-V}_{\text{O}}^z$ complex, the Mn magnetic moment is $4.93 \mu_B$ indicating that the ion has a charge of $2+$ with $S=5/2$. It is interesting that such a result has

been also found experimentally in SrTiO₃ in the cubic phase without charge compensation.¹⁰ In the case of the Mn_{Ti}-V_O^x defects the Mn moment is about 4.9 μ_B consistent with a charge of 2+ and S=5/2. In both cases, the Mn ions maintain their valence states, and their 3d shells are half-filled.

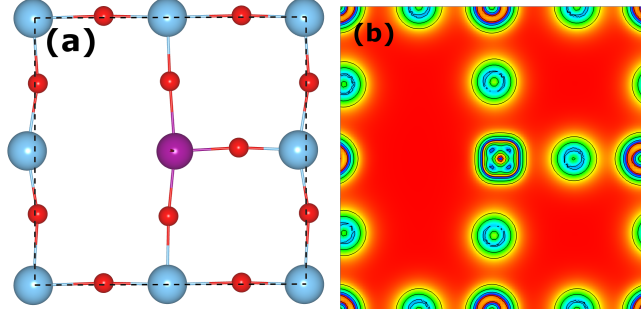


FIG. 5. (color online) (a) The relaxed structure with a Mn_{Ti}-V_O^x defect with a vacancy occupying the nearest equatorial oxygen position, and (b) the corresponding valence charge density.

If the vacancy occupies the nearest equatorial position relative to Mn, both the Mn and Ti atoms move away from the vacancy, see Table I and Fig. 5(a). Again, practically no charge density is detected on the vacancy position, see Fig. 5(b). Since this defect pair is oriented perpendicular to the spontaneous polarization, it is expected to affect ferroelectricity to a lesser extent than when oriented along the *c*-axis.

In summary, depending on the environment, Mn ions in BaTiO₃ can exist in the oxidation states Mn²⁺ and Mn⁴⁺ in agreement with ESR experiments. Their magnetic moments can be either 3 to 5 μ_B . When a Mn impurity goes into the A site in the cubic phase, it is displaced from the A position producing an electric dipole in the highly polarizable media. One can therefore expect that a concentration of such defects in BaTiO₃ will form random electric fields similar to those in Sr_{1-x}Mn_xTiO₃ ceramics.¹² When introduced in the tetragonal phase, Mn_A is also shifted from the initial A position, which further increases the *c/a* ratio. When an Mn goes in the B site, *c/a* and the ferroelectric distortion decrease. The Mn oxygen vacancy complex with the oxygen vacancy on the *c*-axis is favored in energy. In particular, the V_O in the nearest apical position is favored by 0.10 eV as compared to the equatorial one. Therefore, the probability of finding an oxygen vacancy around the Mn center is highest along the polar axis.

This work was supported by the Center the Office of Naval Research (ONR) grants

N00014-12-1-1038 and N00014-14-1-0561 and the European Research Council Advanced Grant ToMCaT. Computations were performed on the DOD High Performance Computing Centers.

- ¹ E. Perez-Delfin, J. E. García, D. A. Ochoa, R. Pérez, F. Guerrero, and J. A. Eiras, *Journal of Applied Physics*, **110**, 034106 (2011).
- ² S. Wu, S. Wang, L. Chen, and X. Wang, *Journal of Materials Science: Materials in Electronics*, **19**, 505 (2008), ISSN 0957-4522.
- ³ J.-H. Park, J. Park, J.-G. Park, B.-K. Kim, and Y. Kim, *Journal of the European Ceramic Society*, **21**, 1383 (2001), ISSN 0955-2219.
- ⁴ M. A. Hentati, M. Guennou, H. Dammak, H. Khemakhem, and M. P. Thi, *Journal of Applied Physics*, **107**, (2010).
- ⁵ H. Neumann and G. Arlt, *Ferroelectrics*, **76**, 303 (1987), ISSN 0015-0193.
- ⁶ G. Arlt and H. Neumann, *Ferroelectrics*, **87**, 109 (1988), ISSN 0015-0193.
- ⁷ X. Ren, *Nat Mater*, **3**, 91 (2004), ISSN 1476-1122.
- ⁸ L. X. Zhang and X. Ren, *Phys. Rev. B*, **71**, 174108 (2005).
- ⁹ L. Zhang and X. Ren, *Phys. Rev. B*, **73**, 094121 (2006).
- ¹⁰ R. A. Serway, W. Berlinger, K. A. Müller, and R. W. Collins, *Phys. Rev. B*, **16**, 4761 (1977).
- ¹¹ T. Kamiya, T. Suzuki, T. Tsurumi, and M. Daimon, *Japanese Journal of Applied Physics*, **31**, 3058 (1992), ISSN 1347-4065.
- ¹² A. Tkach, P. M. Vilarinho, and A. L. Kholkin, *Applied Physics Letters*, **86**, (2005).
- ¹³ A. Tkach, P. Vilarinho, and A. Kholkin, *Acta Materialia*, **54**, 5385 (2006), ISSN 1359-6454.
- ¹⁴ V. V. Laguta, I. V. Kondakova, I. P. Bykov, M. D. Glinchuk, A. Tkach, P. M. Vilarinho, and L. Jastrabik, *Phys. Rev. B*, **76**, 054104 (2007).
- ¹⁵ W. Kleemann, V. V. Shvartsman, S. Bedanta, P. Borisov, A. Tkach, and P. M. Vilarinho, *Journal of Physics: Condensed Matter*, **20**, 434216 (2008), ISSN 0953-8984.
- ¹⁶ V. V. Shvartsman, S. Bedanta, P. Borisov, W. Kleemann, A. Tkach, and P. M. Vilarinho, *Phys. Rev. Lett.*, **101**, 165704 (2008).
- ¹⁷ W. Kleemann, S. Bedanta, P. Borisov, V. V. Shvartsman, S. Miga, J. Dec, A. Tkach, and P. M. Vilarinho, *The European Physical Journal B*, **71**, 407 (2009), ISSN 1434-6028.

- ¹⁸ H. Nakayama and H. Katayama-Yoshida, *Japanese Journal of Applied Physics*, **40**, L1355 (2001).
- ¹⁹ J. Lee, Z. Khim, Y. Park, D. Norton, N. Theodoropoulou, A. Hebard, J. Budai, L. Boatner, S. Pearton, and R. Wilson, *Proceedings of the 9th International Workshop on Oxide Electronics, Solid-State Electronics*, **47**, 2225 (2003), ISSN 0038-1101.
- ²⁰ Y. Shuai, S. Zhou, D. Bürger, H. Reuther, I. Skorupa, V. John, M. Helm, and H. Schmidt, *Journal of Applied Physics*, **109**, 084105 (2011).
- ²¹ J. M. D. Coey, M. Venkatesan, and C. B. Fitzgerald, *Nat Mater*, **4**, 173 (2005), ISSN 1476-1122.
- ²² Y. Yao and H. Fu, *Phys. Rev. B*, **84**, 064112 (2011).
- ²³ E. Cockayne and B. P. Burton, *Phys. Rev. B*, **69**, 144116 (2004).
- ²⁴ L. He and D. Vanderbilt, *Phys. Rev. B*, **68**, 134103 (2003).
- ²⁵ H. Metri, R.-A. Eichel, T. Kloss, K.-P. Dinse, S. Laubach, S. Laubach, P. C. Schmidt, K. A. Schönau, M. Knapp, and H. Ehrenberg, *Phys. Rev. B*, **71**, 134109 (2005).
- ²⁶ R.-A. Eichel, P. Erhart, P. Träskelin, K. Albe, H. Kungl, and M. J. Hoffmann, *Phys. Rev. Lett.*, **100**, 095504 (2008).
- ²⁷ Z. Zhang, P. Wu, L. Lu, and C. Shu, *Applied Physics Letters*, **92**, (2008).
- ²⁸ J. M. Rondinelli, A. S. Eidelson, and N. A. Spaldin, *Phys. Rev. B*, **79**, 205119 (2009).
- ²⁹ S. Bhattacharjee, E. Bousquet, and P. Ghosez, *Phys. Rev. Lett.*, **102**, 117602 (2009).
- ³⁰ H. Sakai, J. Fujioka, T. Fukuda, D. Okuyama, D. Hashizume, F. Kagawa, H. Nakao, Y. Murakami, T. Arima, A. Q. R. Baron, Y. Taguchi, and Y. Tokura, *Phys. Rev. Lett.*, **107**, 137601 (2011).
- ³¹ J. H. Lee and K. M. Rabe, *Phys. Rev. Lett.*, **104**, 207204 (2010).
- ³² O. Kvyatkovskii, *Physics of the Solid State*, **51**, 982 (2009), ISSN 1063-7834.
- ³³ O. Kvyatkovskii, *Physics of the Solid State*, **54**, 1397 (2012), ISSN 1063-7834.
- ³⁴ I. V. Kondakova, R. O. Kuzian, L. Raymond, R. Hayn, and V. V. Laguta, *Phys. Rev. B*, **79**, 134117 (2009).
- ³⁵ R. O. Kuzian, V. V. Laguta, A.-M. Daré, I. V. Kondakova, M. Marysko, L. Raymond, E. P. Garmash, V. N. Pavlikov, A. Tkach, P. M. Vilarinho, and R. Hayn, *EPL (Europhysics Letters)*, **92**, 17007 (2010), ISSN 0295-5075.
- ³⁶ G. Xavier, *Zeitschrift für Kristallographie*, **220**, 558 (2009).
- ³⁷ X. Gonze, B. Amadon, P.-M. Anglade, J.-M. Beuken, F. Bottin, P. Boulanger, F. Bruneval,

- D. Caliste, R. Caracas, M. Côté, T. Deutsch, L. Genovese, P. Ghosez, M. Giantomassi, S. Goedecker, D. Hamann, P. Hermet, F. Jollet, G. Jomard, S. Leroux, M. Mancini, S. Mazevet, M. Oliveira, G. Onida, Y. Pouillon, T. Rangel, G.-M. Rignanese, D. Sangalli, R. Shaltaf, M. Torrent, M. Verstraete, G. Zerah, and J. Zwanziger, *40 YEARS OF CPC: A celebratory issue focused on quality software for high performance, grid and novel computing architectures*, Computer Physics Communications, **180**, 2582 (2009), ISSN 0010-4655.
- ³⁸ Z. Wu and R. E. Cohen, Phys. Rev. B, **73**, 235116 (2006).
- ³⁹ R. E. Cohen, I. I. Mazin, and D. G. Isaak, Science, **275**, 654 (1997).
- ⁴⁰ J. Kunes, A. V. Lukoyanov, V. I. Anisimov, R. T. Scalettar, and W. E. Pickett, Nat Mater, **7**, 198 (2008), ISSN 1476-1122.
- ⁴¹ K. Müller, W. Berlinger, K. Blazey, and J. Albers, Solid State Communications, **61**, 21 (1987), ISSN 0038-1098.
- ⁴² G. Völkel and K. A. Müller, Phys. Rev. B, **76**, 094105 (2007).
- ⁴³ V. V. Laguta, M. D. Glinchuk, I. P. Bykov, Y. L. Maksimenko, J. Rosa, and L. Jastrabk, Phys. Rev. B, **54**, 12353 (1996).